

International Journal of Modern Physics A  
 © World Scientific Publishing Company

## Cosmogenic activation of materials

Susana Cebrián

*Grupo de Física Nuclear y Astropartículas,  
 Universidad de Zaragoza, Calle Pedro Cerbuna 12, 50009 Zaragoza, Spain  
 Laboratorio Subterráneo de Canfranc, Paseo de los Ayerbe s/n  
 22880 Canfranc Estación, Huesca, Spain  
 scebrian@unizar.es*

Received Day Month Year  
 Revised Day Month Year

Experiments looking for rare events like the direct detection of dark matter particles, neutrino interactions or the nuclear double beta decay are operated deep underground to suppress the effect of cosmic rays. But the production of radioactive isotopes in materials due to previous exposure to cosmic rays is a hazard when ultra-low background conditions are required. In this context, the generation of long-lived products by cosmic nucleons has been studied for many detector media and for other materials commonly used. Here, the main results obtained on the quantification of activation yields on the Earth's surface will be summarized, considering both measurements and calculations following different approaches. The isotope production cross sections and the cosmic ray spectrum are the two main ingredients when calculating this cosmogenic activation; the different alternatives for implementing them will be discussed. Activation that can take place deep underground mainly due to cosmic muons will be briefly commented too. Presently, the experimental results for the cosmogenic production of radioisotopes are scarce and discrepancies between different calculations are important in many cases, but the increasing interest on this background source which is becoming more and more relevant can help to change this situation.

*Keywords:* Activation; cosmic rays; radioactive background; dark matter; neutrino.

PACS numbers: 13.85.Tp; 23.40.-s; 25.40.-h; 25.30.Mr; 95.35.+d

### 1. Introduction

Experiments searching for rare phenomena like the interaction of Weakly Interacting Massive Particles (WIMPs) which could be filling the galactic dark matter halo, the detection of elusive neutrinos or the nuclear double beta decay of some nuclei require detectors working in ultra-low background conditions and taking data for very long periods of time at the scale of a few years due to the extremely low counting rates expected. Operating in deep underground locations, using active and passive shields and selecting carefully radiopure materials reduce very efficiently the background for this kind of experiments.<sup>1,2</sup> In this context, long-lived radioactive impurities in the materials of the set-up induced by the exposure to cosmic rays

2 *S. Cebrián*

at sea level (during fabrication, transport and storage) may be even more important than residual contamination from primordial radionuclides and become very problematic. For instance, the poor knowledge of cosmic ray activation in detector materials is highlighted in Ref. 3 as one of the three main uncertain nuclear physics aspects of relevance in the direct detection approach pursued to solve the dark matter problem. Production of radioactive isotopes by exposure to cosmic rays is a well known issue<sup>4,5</sup> and several cosmogenic isotopes are important in extraterrestrial and terrestrial studies in many different fields, dealing with astrophysics, geophysics, paleontology and archaeology.

One of the most relevant processes in the cosmogenic production of isotopes is the spallation of nuclei by high energy nucleons, but other reactions like fragmentation, induced fission or capture can be very important for some nuclei. Since protons are absorbed by the atmosphere, nuclide production is mainly dominated by neutrons at the Earth's surface, but if materials are flown at high altitudes, in addition to the fact that the cosmic flux is much greater, protons will produce significant activation as well.

In principle, cosmogenic activation can be kept under control by minimizing exposure at surface and storing materials underground, avoiding flights and even using shields against the hadronic component of cosmic rays during surface detector building or operation. In addition, purification techniques could help reducing the produced background isotopes. But since these requirements usually complicate the preparation of experiments (for example, while crystal growth and detector mounting steps) it would be desirable to have reliable tools to quantify the real danger of exposing the different materials to cosmic rays. Production rates of cosmogenic isotopes in all the materials present in the experimental set-up, as well as the corresponding cosmic rays exposure history, must be both well known in order to assess the relevance of this effect in the achievable sensitivity of an experiment. Direct measurements, by screening of exposed materials in very low background conditions as those achieved in underground laboratories, and calculations of production rates and yields, following different approaches, have been made for several materials in the context of dark matter, double beta decay and neutrino experiments. Many different studies are available for germanium and interesting results have been derived in the last years also for other detector media like tellurium and tellurium oxide, sodium iodide, xenon, argon or neodymium as well as for materials commonly used in the set-ups like copper, lead, stainless steel or titanium (see for instance the summaries in Refs. 6, 7). However, systematic studies for other targets are missed.

The relevant long-lived radioactive isotopes cosmogenically induced are in general different for each target material, although there are some common dangerous products like tritium, because being a spallation product, it can be generated in any material. Tritium is specially relevant for dark matter experiments for its decay properties (it is a pure beta emitter with transition energy of 18.591 keV and a long half-life of 12.312 y<sup>8</sup>) when induced in the detector medium. Quantifica-

tion of tritium cosmogenic production is not easy, neither experimentally since its beta emissions are hard to disentangle from other background contributions, nor by calculations, as tritium can be produced by different reaction channels.

The aim of this work is to summarize and compare the main results obtained for estimating the activation yields of relevant long-lived radioactive isotopes due to cosmic nucleons on the Earth's surface in the materials of interest for rare event experiments, taken into consideration both measurements and calculations. The structure of the paper is as follows. First, section 2 describes the relevant calculation tools available. Activation results derived for different detector media are summarized in the following sections, including semiconductor materials like germanium (section 3) and silicon (section 4), tellurium used in different detectors (section 5), scintillators like sodium iodide (section 6) and noble liquid-gas detectors as xenon (section 7) and argon (section 8). The production of cosmogenic isotopes in other materials typically used in experiments is also considered, in particular, for copper (section 9), lead (section 10), stainless steel (section 11) and titanium (section 12). Results for other targets are collected in section 13. For each material, the available estimates of production rates of the relevant radionuclides will be presented, emphasizing the comparison with experimental results whenever possible. Some results concerning the activation of materials underground are mentioned too in section 14 before the final summary.

## 2. Calculation Tools

The activity  $A$  of a particular isotope with decay constant  $\lambda$  induced in a material must be evaluated taking into account the time of exposure to cosmic rays ( $t_{exp}$ ), the cooling time corresponding to the time spent underground and sheltered from cosmic rays ( $t_{cool}$ ) and the production rate  $R$ :

$$A = R[1 - \exp(-\lambda t_{exp})] \exp(-\lambda t_{cool}). \quad (1)$$

As it will be shown in the next sections, there are some direct measurements of productions rates in some materials as the saturation activity, but unfortunately they are not very common. Consequently, in many cases production rates have to be estimated from two basic energy-dependent ingredients, the flux  $\phi$  of cosmic rays and the cross-section  $\sigma$  of isotope production:

$$R = N \int \sigma(E) \phi(E) dE. \quad (2)$$

$N$  being the number of target nuclei and  $E$  the particle energy.

The excitation function for the production of a certain isotope by nucleons in a target over a wide range of energies (typically from some MeV up to several GeV) can be hardly obtained experimentally, since the measurements of production cross-sections with beams are long, expensive and there are not many available facilities

to carry them out. The use of computational codes to complete information on the excitation functions is therefore mandatory. In addition, measurements are usually performed on targets with the natural composition of isotopes for a given element, often determining only cumulative yields of residual nuclei. Reliable calculations are required to provide independent yields for isotopically separated targets if necessary. But in any case, experimental data are essential to check the reliability of calculations. The suitability of a code to a particular activation problem depends on energy, targets and projectiles to be considered. Some systematic and extensive comparisons of calculations and available measurements have been made based on analysis of deviation factors  $F$ , defined as:

$$F = 10^{\sqrt{d}}, \quad d = \frac{1}{n} \sum_i (\log \sigma_{exp,i} - \log \sigma_{cal,i})^2 \quad (3)$$

$n$  being the number of pairs of experimental and calculated cross sections  $\sigma_{exp,i}$  and  $\sigma_{cal,i}$  at the same energies.

There are several possibilities to obtain values of **production cross sections**:

- Experimental results can be found at EXFOR database (CSISRS in USA),<sup>9</sup> an extensive compilation of nuclear reaction data from thousands of experiments. Available data for a particular target, projectile, energy or reaction can be easily searched for by means of a public web form. NUCLEX<sup>10</sup> is also a compilation of experimental data.
- Semiempirical formulae were deduced for nucleon-nucleus cross sections for different reactions (break-up, spallation, fission, . . .) exploiting systematic regularities and tuning parameters to best fit available experimental results. The famous Silberberg&Tsao equations<sup>11–15</sup> can be applied for light and heavy targets ( $A \geq 3$ ), for a wide range of product radionuclides ( $A \geq 6$ ) and at energies above 100 MeV. These equations have been implemented in different codes, which offer very fast calculations in contrast to Monte Carlo simulations:
  - (a) COSMO<sup>16</sup> is a FORTRAN program with three modes of calculation: excitation curve of a nuclide for a specified target, mass yield curve for given target and energy and final activities produced for a target exposed to cosmic rays. It allows a complete treatment for targets with  $A < 210$  and  $Z < 83$ .
  - (b) YIELDX<sup>15</sup> is a FORTRAN routine to calculate the production cross-section of a nuclide in a particular target at a certain energy. It includes the latest updates of the Silberberg & Tsao equations.
  - (c) ACTIVIA<sup>17</sup> is C++ computer package to calculate target-product cross sections as well as production and decay yields from cosmic ray activation. It uses semiempirical formulae but also experimental data tables if available.

The main limitation of the formulae is that they are based only on proton-induced reactions; therefore, the fact that cross sections are equal for neutrons and protons has to be assumed.

- Monte Carlo simulation of the hadronic interaction between nucleons and nuclei can output also production cross sections. Modeling isotope production includes a wide range of reactions: the formation and decay of a long-lived compound nucleus at low energies, while in the GeV range the intranuclear cascade (INC) of nucleon-nucleon interactions is followed by different deexcitation processes (spallation, fragmentation, fission, . . .). Many different models and codes implementing them have been developed in very different contexts (studies of cosmic rays and astrophysics, transmutation of nuclear waste or production of medical radioisotopes for instance): BERTINI, ISABEL, LAHET, GEM, TALYS, HMS-ALICE, INUCL, LAQGSM, CEM, ABLA, CASCADE, MARS, SHIELD, . . . are the names of just a few of them. Some of these models have been integrated in general-purpose codes like GEANT4,<sup>18</sup> FLUKA<sup>19</sup> and MCNP.<sup>20</sup> In Ref. 21, the capabilities of GEANT4 and MCNPX to simulate neutron spallation were studied; in particular, the neutron multiplicity predicted was compared with measurements finding some discrepancies for low density materials. In Ref. 22 preferred models for each target mass range are selected, for neutron and proton-induced reactions while in Ref. 23 it is concluded that versions of CEM03 and INCL+ABLA codes can be considered as the most accurate. A relevant advantage of Monte Carlo codes is that they are applicable not only to proton-induced but also to neutron-induced nuclear reactions.
- Several libraries of production cross sections have been prepared combining calculations and experimental data, with different coverage of energies, projectiles and reactions:
  - (a) RNAL (Reference Neutron Activation Library)<sup>24</sup> is restricted to 255 reactions.
  - (b) LA150<sup>25</sup> contains results up to 150 MeV, independently for neutrons and protons as projectiles, using calculations from HMS-ALICE.
  - (c) MENDL-2 and MENDL-2P (Medium Energy Nuclear Data Library)<sup>26</sup> are based on calculations using codes of the ALICE family, containing excitation functions which cover a very wide range of target and product nuclides, either for neutrons or protons, for energies up to 100 MeV for neutrons (MENDL-2, using ALICE92) and 200 MeV for protons (MENDL-2P, using ALICEIPPE).
  - (d) TENDL (TALYS-based Evaluated Nuclear Data Library)<sup>27</sup> offers cross sections obtained with the TALYS nuclear model code system for neutrons and protons up to 200 MeV for all the targets.
  - (e) An evaluated library for neutrons and protons to 1.7 GeV was presented in Ref. 28. It gives excitation functions including available experimental data and calculated results using CEM95, LAHET, and HMS-ALICE codes for selected targets and products.
  - (f) HEAD-2009 (High Energy Activation Data)<sup>22</sup> is a complete compilation of data for neutrons and protons from 150 MeV up to 1 GeV. The choice of models was dictated by an extensive comparison with EXFOR data. In par-

ticular, in HEPAD-2008 (High-Energy Proton Activation Data) sub-library cross sections are obtained using a selection of models and codes like CEM 03.01, CASCADE/INPE and MCNPX 2.6.0. Only targets with  $Z \geq 12$  are considered.

The detailed studies of excitation functions performed in different areas, like Positron Emission Tomography (PET) nuclear medicine imaging process, for different targets and products and based on irradiation experiments and several types of calculations (see for example recent works from Refs. 29–34), can serve as a reference to select the most adequate libraries or packages.

Relevant activation processes on the Earth's surface are induced mainly by nucleons at MeV-GeV energy range. At sea level, the flux of neutrons and protons is virtually the same at energies of a few GeV; however, at lower energies the proton to neutron ratio decreases significantly because of the absorption of charged particles in the atmosphere. For example, at 100 MeV this ratio is about 3%.<sup>4</sup> Consequently, neutrons dominate the contribution to the **cosmic ray spectrum** to be considered at sea level. But it must be kept in mind that proton activation, being much smaller, is not completely negligible. The typical contribution from protons to isotope production is quoted as  $\sim 10\%$  of the total in Ref. 4, which agrees for instance with the results in Refs. 35, 36 where proton activation in germanium was specifically evaluated for some isotopes. Concerning activation by other cosmic particles like muons, it is even smaller, as confirmed by calculations in Refs. 36, 37.

Different forms of the neutron spectrum at sea level have been used in cosmogenic activation studies, like the Hess<sup>38</sup> and Lal&Peters<sup>4</sup> spectra. The ACTIVIA code uses the energy spectrum from parameterizations in Refs. 39, 40. In Ref. 41, a compilation of measurements was made, including the historical Hess spectrum and relevant corrections, and an analytic function valid from 10 MeV to 10 GeV was derived. In Ref. 42 a set of measurements of cosmic neutrons on the ground across the USA was accomplished using Bonner sphere spectrometers; a different analytic expression fitting data for energies above 0.4 MeV was proposed (referred hereafter as Gordon et al. spectrum). Just to appreciate the difference between different spectra, three considered parameterizations are compared in Fig. 1, applied for the conditions of New York City at sea level; the integral flux from 10 MeV to 10 GeV is  $5.6 \times 10^{-3} \text{cm}^{-2} \text{s}^{-1}$  for Ref. 41 and  $3.6 \times 10^{-3} \text{cm}^{-2} \text{s}^{-1}$  for Ref. 42. The Gordon et al. parametrization gives a lower neutron flux above 1000 MeV. To evaluate the activation at a particular location, the relative neutron flux to the sea-level flux in New York City can be determined using the calculator available in Ref. 43.

For surface protons, the energy spectrum from Ref. 44 can be used; the total flux corresponding to the energy range from 100 MeV to 100 GeV is  $1.358 \times 10^{-4} \text{cm}^{-2} \text{s}^{-1}$ . It is worth noting that in Ref. 45, the energy spectra at sea level for different particles including neutrons, protons and muons have been generated from Monte Carlo simulation of primary protons implementing a model of the Earth's atmosphere in different codes, finding a satisfactory agreement between

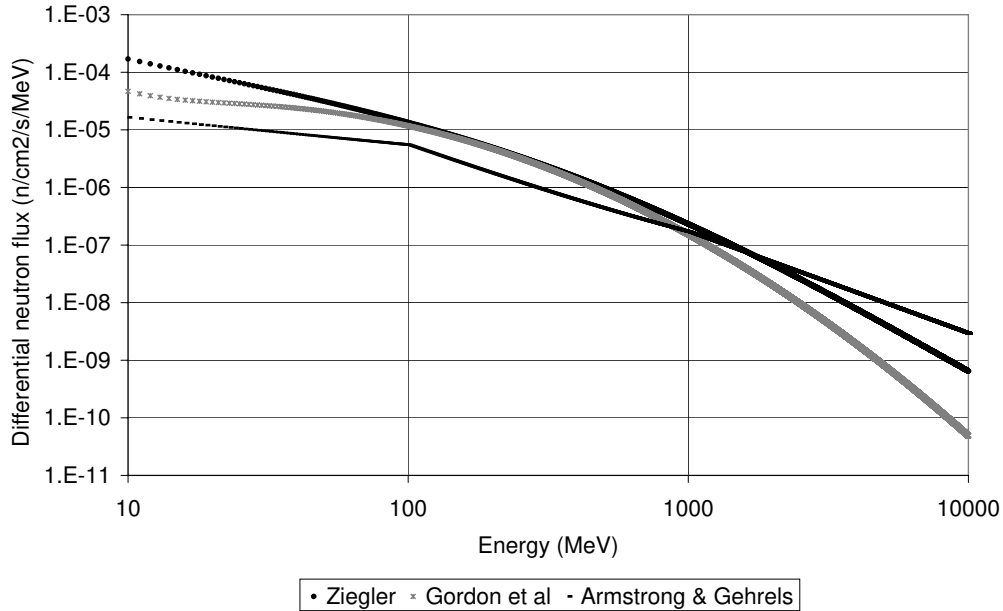


Fig. 1. Differential flux of cosmic neutrons at sea level, using the parameterizations from Armstrong and Gehrels,<sup>39,40</sup> Ziegler<sup>41</sup> and Gordon et al.<sup>42</sup>

codes and available data. Therefore, it seems that Monte Carlo calculations could provide too quite reliable predictions of cosmic-ray distributions at sea level.

### 3. Germanium

A great deal of experiments and projects looking for rare events (like the interaction of dark matter or the double beta decay of  $^{76}\text{Ge}$ ) have used or are using germanium crystals either as conventional diodes (like IGEX,<sup>46</sup> Heidelberg-Moscow,<sup>47</sup> GERDA,<sup>48</sup> MAJORANA,<sup>49</sup> CoGENT,<sup>50</sup> TEXONO or CDEX<sup>51</sup>) or as cryogenic detectors (like CDMS<sup>52</sup> or EDELWEISS<sup>53</sup>). Therefore, many different activation studies have been performed for germanium. The observation for the first time of several cosmogenic isotopes through low energy peaks produced due to their decay by electron capture in the crystals of the CoGENT experiment was reported in Ref. 50 and cosmogenic products are usually considered in the background models of experiments.<sup>54</sup> In this section, the main results obtained for quantifying the cosmogenic yields in both natural and enriched<sup>a</sup> germanium are summarized.

<sup>a</sup>Typical isotopic composition of enriched germanium used in double beta decay searches is 86% of  $^{76}\text{Ge}$  and 14% of  $^{74}\text{Ge}$ .

- Early estimates of production rates of induced isotopes were made in Refs. 55, 56 using excitation functions calculated with the spallation reaction code LAHET/ISABEL and the Hess and Lal&Peters neutron spectra. Production rates were also derived experimentally in Homestake and Canfranc laboratories from germanium detectors previously exposed.<sup>55</sup> Agreement with calculation was within a factor of 2 and in some cases within 30%.
- Productions of cosmogenic isotopes was assessed in Ref. 57 using a semiempirical code named  $\Sigma$ .
- Production cross sections were measured irradiating at Los Alamos Neutron Science Center (LANSCE) a natural germanium target with a proton beam with an energy of 800 MeV.<sup>58</sup> Screening with germanium detectors was performed at Berkeley intermittently from 2 weeks to 5 years after irradiation. A quite good agreement with predictions of Silberberg&Tsao formulae was obtained.
- Estimates of production rates for  $^{60}\text{Co}$  and  $^{68}\text{Ge}$  were made using excitation functions calculated with the SHIELD code in Ref. 35. It is worth noting than in this estimate rates were evaluated including not only the neutron but also the proton contribution; as mentioned in section 2, the latter amounts around a  $\sim 10\%$  of the total.
- The ACTIVIA code, including the energy spectrum for cosmic ray neutrons at sea level based on the parametrization from Armstrong<sup>39</sup> and Gehrels<sup>40</sup> was used to evaluate production rates in both natural and enriched germanium for benchmark.<sup>17</sup>
- Another estimate of relevant production rates can be found in Ref. 59. Excitation functions were calculated using the TALYS code and the neutron spectrum was considered from the Gordon et al. parametrization.
- In Ref. 60, a 11-g sample of enriched germanium was exposed at LANSCE to a wide-band pulsed neutron beam that resembles the cosmic-ray neutron flux, with energies up to about 700 MeV. After cooling, germanium gamma counting was performed underground at the Waste Isolation Pilot Plant (WIPP) for 49 days to evaluate the nuclei production. This production was also predicted by calculating cross sections with CEM03 code. Calculations seem to overestimate production in a factor of 3 depending on isotope. In addition, measured yields were converted to cosmogenic production rates considering the Gordon et al. neutron spectrum.
- An estimate of production rates after a careful evaluation of excitation functions was presented in Ref. 61. Information on excitation functions for each relevant isotope was collected searching for experimental data (available only for protons) and available calculations (MENDL libraries<sup>26</sup> and other ones based on different codes<sup>28</sup>) and performing some new calculations (using YIELDX). Then, deviation factors were evaluated between measured cross sections and different calculations and the selected description of the excitation functions was the following: HMS-ALICE calculations for neutrons below 150 MeV and YIELDX results above this energy. Production rates were computed for both the Ziegler and Gordon et al. spectra. It was checked that, in general, estimates based on the Gordon et



al. spectrum are closer to available experimental results; the uncertainty in the activation yields coming from the cosmic ray flux was for most of the analyzed products below a factor 2.

- Neutron irradiation experiments have been performed on enriched germanium to determine the neutron radiative-capture cross sections on  $^{74}\text{Ge}$  and  $^{76}\text{Ge}$ , for neutron thermal energies<sup>62,63</sup> and energies of the order of a few MeV.<sup>64</sup> These results are of special interest for double beta decay experiments like GERDA and MAJORANA. Neutron capture results in a cascade of prompt de-excitation gamma rays from excited states of produced nucleus and the emissions from the decay of this nucleus, if it is radioactive.
- Recently, a precise quantification of cosmogenic products in natural germanium including tritium has been made by the EDELWEISS III direct dark matter search experiment,<sup>65</sup> following a detailed analysis of a long measurement with many germanium detectors with different exposures to cosmic rays. The cosmogenic yields are evaluated by fitting the measured data in the low energy region to a continuum level plus several peaks at the binding energies of electrons in K and L shells, corresponding to different isotopes decaying by electron capture. The decay rates measured in detectors are converted into production rates, considering their well-known exposure history above ground during different steps of production and shipment. Estimates of the production rates calculated with the ACTIVIA code (modified to consider the Gordon et al. cosmic neutron spectrum) are also presented in Ref. 65 for comparison.
- Presence of tritium in the germanium detectors of the MAJORANA DEMONSTRATOR focused on the study of the double beta decay has been reported too.<sup>49</sup> A first estimate of the production rate of several radioisotopes in enriched germanium, including tritium, from the data of the MAJORANA DEMONSTRATOR has been very recently presented.<sup>66</sup> These enriched detectors (having 87% of  $^{76}\text{Ge}$  and 13% of  $^{74}\text{Ge}$ ) have a very well-known exposure history. The fitting model to derive the abundance of cosmogenic products is comprised of a calculated tritium beta-decay spectrum, flat background, and multiple X-ray peaks.
- A detailed study of the impact of cosmogenic activation in natural and enriched germanium has been carried out in Ref. 36, estimating the production rates of many isotopes including tritium not only for dominating neutrons but also for protons and muons, using Geant4 simulations and ACTIVIA calculations. In addition, the effect of a shielding against activation has been analyzed and the expected background rates in the regions of interest have been evaluated for particular exposure and cooling conditions. All results from this work considered here correspond to neutron activation using the Gordon et al. spectrum.

Tables 1 and 2 summarize the rates of production (expressed in  $\text{kg}^{-1} \text{d}^{-1}$ ) of some of the isotopes induced in natural and enriched germanium at sea level obtained either from measurements or from calculations based on the different approaches described before. Experimental results quoted in Ref. 1 are also included.

Table 1. Production rates (in  $\text{kg}^{-1} \text{d}^{-1}$ ) at sea level for isotopes induced in natural germanium following measurements in Refs. 55,65 and different calculations (see text).

|                                  | $^{49}\text{V}$ | $^{54}\text{Mn}$ | $^{55}\text{Fe}$ | $^{57}\text{Co}$ | $^{58}\text{Co}$ | $^{60}\text{Co}$ | $^{65}\text{Zn}$ | $^{68}\text{Ge}$ |
|----------------------------------|-----------------|------------------|------------------|------------------|------------------|------------------|------------------|------------------|
| Half-life <sup>67,68</sup>       | 330 d           | 312.19 d         | 2.747 y          | 271.82 d         | 70.85 d          | 5.2711 y         | 244.01 d         | 270.95 d         |
| Measurement <sup>55</sup>        |                 | 3.3±0.8          |                  | 2.9±0.4          | 3.5±0.9          |                  | 38±6             | 30±7             |
| Measurement <sup>65</sup>        | 2.8±0.6         |                  | 4.6±0.7          |                  |                  |                  | 106±13           | >74              |
| Monte Carlo <sup>55</sup>        |                 | 2.7              |                  | 4.4              | 5.3              |                  | 34.4             | 29.6             |
| Monte Carlo <sup>56</sup>        |                 |                  |                  | 0.5              | 4.4              | 4.8              | 30.0             | 26.5             |
| Sigma <sup>57</sup>              |                 | 9.1              | 8.4              | 10.2             | 16.1             | 6.6              | 79.0             | 58.4             |
| SHIELD <sup>35</sup>             |                 |                  |                  |                  |                  | 2.9              |                  | 81.6             |
| ACTIVIA <sup>17</sup>            |                 | 2.7              | 3.4              | 6.7              | 8.5              | 2.8              | 29.0             | 45.8             |
| TALYS <sup>59</sup>              |                 | 2.7              | 8.6              | 13.5             |                  | 2.0              | 37.1             | 41.3             |
| MENDL+YIELDX <sup>61</sup>       |                 | 5.2              | 6.0              | 7.6              | 10.9             | 3.9              | 63               | 60               |
| ACTIVIA <sup>65</sup>            | 1.9             |                  | 3.5              |                  |                  |                  | 38.7             | 23.1             |
| ACTIVIA (MENDL-2P) <sup>65</sup> | 1.9             |                  | 4.0              |                  |                  |                  | 65.8             | 45.0             |
| GEANT4 <sup>36</sup>             |                 | 2.0              | 7.9              | 7.4              | 5.7              | 2.9              | 75.9             | 182.8            |
| ACTIVIA <sup>36</sup>            |                 | 2.8              | 4.1              | 8.9              | 11.4             | 4.1              | 44.2             | 24.7             |

 Table 2. Production rates (in  $\text{kg}^{-1} \text{d}^{-1}$ ) at sea level for isotopes induced in enriched germanium (86-87% of  $^{76}\text{Ge}$  and 14-13% of  $^{74}\text{Ge}$ ) following measurements quoted in Refs. 1,60,66 and different calculations (see text).

|                            | $^{54}\text{Mn}$ | $^{55}\text{Fe}$ | $^{57}\text{Co}$ | $^{58}\text{Co}$ | $^{60}\text{Co}$ | $^{65}\text{Zn}$ | $^{68}\text{Ge}$ |
|----------------------------|------------------|------------------|------------------|------------------|------------------|------------------|------------------|
| Half-life <sup>67,68</sup> | 312.19 d         | 2.747 y          | 271.82 d         | 70.85 d          | 5.2711 y         | 244.01 d         | 270.95 d         |
| Measurement <sup>1</sup>   | 2.3              |                  | 1.6              | 1.2              |                  | 11               |                  |
| Measurement <sup>60</sup>  | 2.0±1.0          |                  | 0.7±0.4          |                  | 2.5±1.2          | 8.9±2.5          | 2.1±0.4          |
| Measurement <sup>66</sup>  | 4.4±4.1          | 2.1±0.7          |                  |                  |                  | 4.3±3.6          | 3.3±1.6          |
| Monte Carlo <sup>55</sup>  | 1.4              |                  | 1                | 1.8              |                  | 6.4              | 0.94             |
| Monte Carlo <sup>56</sup>  |                  |                  | 0.08             | 1.6              | 3.5              | 6.0              | 1.2              |
| SHIELD <sup>35</sup>       |                  |                  |                  |                  | 3.3              |                  | 5.8              |
| ACTIVIA <sup>17</sup>      | 2.2              | 1.6              | 2.9              | 5.5              | 2.4              | 10.4             | 7.6              |
| TALYS <sup>59</sup>        | 0.87             | 3.4              | 6.7              |                  | 1.6              | 20               | 7.2              |
| MENDL+YIELDX <sup>61</sup> | 3.7              | 1.6              | 1.7              | 4.6              | 5.1              | 20               | 12               |
| GEANT4 <sup>36</sup>       | 1.4              | 4.5              | 3.3              | 2.9              | 2.4              | 24.9             | 21.8             |
| ACTIVIA <sup>36</sup>      | 2.2              | 1.2              | 2.3              | 5.5              | 4.4              | 9.7              | 15.4             |

When comparing all the available results for germanium, the order of magnitude of measured values is reasonably reproduced by calculations, but there is an important dispersion in results for some isotopes which can be very relevant, like  $^{68}\text{Ge}$ . In enriched germanium, cosmogenic activation is significantly suppressed for most of the isotopes.

As pointed out before, germanium is being used as a target for dark matter searches for many years, either as pure ionization detectors or in cryogenic detectors measuring simultaneously ionization and heat. The production of tritium in the detector media can be specially worrisome due to its emissions. A part of the unexplained background in the low energy region of the IGEX detectors could be attributed to tritium<sup>69</sup> and tritium is highlighted as one the relevant background

Table 3. Production rates (in  $\text{kg}^{-1}\text{d}^{-1}$ ) of  $^3\text{H}$  at sea level evaluated for several targets from measurements or calculations based on different approaches (see text). The two values from Ref. 55 were derived using different neutron spectra and the two values from ACTIVIA in Ref. 65 correspond to using just semiempirical cross sections or data from MENDL-2P too.

| Target                        | Ref. 55 | TENDL+HEAD <sup>71</sup> | TALYS <sup>59</sup> | GEANT4 <sup>37</sup> | GEANT4 <sup>36</sup> | ACTIVIA <sup>37</sup> | ACTIVIA <sup>36</sup> | ACTIVIA               | Others                                    |
|-------------------------------|---------|--------------------------|---------------------|----------------------|----------------------|-----------------------|-----------------------|-----------------------|---|
| <i>nat</i> Ge                 | 178/210 | 75±26                    | 27.7                | 48.3                 | 47.4                 | 52.4                  | 52.4                  | 46/43.5 <sup>65</sup> | 82±21 <sup>65</sup><br>76±6 <sup>70</sup> |
| <i>enr</i> Ge                 | 113/140 | 94±34                    | 24.0                |                      | 47.4                 |                       | 51.3                  |                       | 140±10 <sup>66</sup>                      |
| Si                            |         |                          |                     | 27.3                 |                      | 108.7                 |                       |                       | 125 <sup>52</sup>                         |
| TeO <sub>2</sub>              |         |                          | 43.7                |                      |                      |                       |                       |                       |   |
| NaI                           |         | 83±27                    | 31.1                | 42.9                 |                      | 36.2                  |                       | 26 <sup>90</sup>      |   |
| CsI                           |         |                          | 19.7                |                      |                      |                       |                       |                       |   |
| CaWO <sub>4</sub>             |         |                          | 45.5                |                      |                      |                       |                       |                       |   |
| Ar                            |         | 146±31                   | 44.4                | 84.9                 |                      | 82.9                  |                       |                       |   |
| Ne                            |         | 228±16                   |                     |                      |                      |                       |                       |                       |   |
| Xe                            |         |                          | 16.0                | 31.6                 |                      | 35.6                  |                       |                       |   |
| Quartz                        |         |                          |                     |                      |                      |                       |                       | 46 <sup>90</sup>      |   |
| C <sub>2</sub> H <sub>6</sub> |         |                          |                     | 279.5                |                      |                       |                       |                       |   |

sources in future experiments like SuperCDMS.<sup>52</sup> Indeed, the first experimental estimates of the tritium production rate in germanium at sea level have been derived by the EDELWEISS collaboration<sup>65</sup> for natural germanium and using data from the MAJORANA DEMONSTRATOR<sup>66</sup> for enriched germanium; a new estimate based on CDMSlite data<sup>70</sup> has been also presented. Several calculations had been made before: a rough calculation was attempted in Ref. 55 using two different neutron spectra. This was followed by other estimates based in TALYS<sup>59</sup> and ACTIVIA and GEANT4,<sup>36,37</sup> profiting from the availability of reaction codes that fully identify all the reaction products in the final state. In Ref. 71, dedicated calculations of production rates of tritium at sea level have been performed for some of the materials typically used as targets in dark matter detectors (germanium, sodium iodide, argon and neon), based on a selection of excitation functions over the entire energy range of cosmic neutrons, mainly from TENDL for neutrons and HEAD-2009 libraries. All these results on the production rate of tritium in both natural and enriched germanium are summarized in Table 3. An additional estimate of the production rate in enriched germanium using the COSMO code gives  $70 \text{ kg}^{-1} \text{ d}^{-1}$ .<sup>69</sup> For the natural material, calculations give in general lower values than the measured rates; in particular, the smallest value from<sup>59</sup> can be understood because using TALYS cross-sections only contributions from the lowest energy neutrons are considered. The range derived in Ref. 71 is well compatible with the measured rates by EDELWEISS and CDMSlite. For enriched germanium, as used in double beta decay experiments, the measured production rate is higher than in natural germanium; this can be due to the fact that cross sections increase with the mass number of the germanium isotope in all the energy range above  $\sim 50 \text{ MeV}$ , according to TENDL-2013 and HEAD-2009 data.<sup>71</sup>

In addition to the quantification of the cosmogenic activation, the effect of this

activity in germanium detectors has been studied too.<sup>36</sup> In Ref. 72, a background simulation method for cosmogenic radionuclides inside HPGe detectors for rare event experiments is presented, to quantify the expected spectrum for each internal cosmogenic isotope analyzing phenomena caused by the coincidence summing-up effect.

#### 4. Silicon

Silicon is the detector medium in cryogenic detectors, like those of the CDMS experiment, or in CCD detectors, used in the DAMIC experiment,<sup>73</sup> both devoted to the direct detection of dark matter. The intrinsic isotope  $^{32}\text{Si}$ , a  $\beta^-$  emitter with an endpoint energy of 224.5 keV and half-life of 150 y,<sup>67</sup> can be a relevant background source. It is produced as a spallation product from cosmic ray secondaries on argon in the atmosphere;  $^{32}\text{Si}$  atoms can make their way into the terrestrial environment through aqueous transport and therefore its concentration can depend on the exact source and location of the silicon used in the production and fabrication of detectors. A decay rate of  $80_{-65}^{+110} \text{ kg}^{-1} \text{ d}^{-1}$  has been found by the DAMIC collaboration in their CCD detectors<sup>74</sup> and this isotope is considered in the estimates of SuperCDMS sensitivity.<sup>52</sup>

Also tritium can be relevant for silicon detectors, as pointed out in Ref. 52. An estimate of the production rate based on GEANT4 and ACTIVIA (using the Gordon et al. neutron spectrum) is presented in Ref. 37 and results are shown in Table 3, together with the production rate considered by the SuperCDMS collaboration.<sup>52</sup>

#### 5. Tellurium

Activation in tellurium has been mainly studied with focus on the CUORE<sup>75</sup> and SNO+<sup>76</sup> double beta decay experiments. The production rate of tritium in  $\text{TeO}_2$  was also evaluated using the TALYS code<sup>59</sup> and it is reported in Table 3.

Results for proton production cross sections obtained within the CUORE project were published in Ref. 77, completing previous results on proton spallation reactions on tellurium.<sup>58,78</sup> Some measurements were made in USA, by irradiating a tellurium target with the 800 MeV proton beam at LANSCE and performing a gamma screening with germanium detectors in Berkeley. Other measurements were carried out in Europe, exposing  $\text{TeO}_2$  targets to proton beams with energies of 1.4 and 23 GeV at CERN; first germanium screening was made there for several months and later in Milano 2.8 and 4.6 years after irradiation. The obtained cross sections at the three energies are in good agreement with Silberberg&Tsao predictions. In addition, as presented in Ref. 79, flux-averaged cross-sections for neutron activation in natural tellurium were measured by irradiating at LANSCE  $\text{TeO}_2$  powder with the neutron beam containing neutrons of kinetic energies up to  $\sim 800$  MeV and having an energy spectrum similar to that of cosmic-ray neutrons at sea-level; gamma ray analysis was performed in Berkeley Low Background Facility. The cross sections obtained for  $^{110m}\text{Ag}$  and  $^{60}\text{Co}$ , the two isotopes identified as the most relevant ones

Table 4. Production rates (in  $\mu\text{Bq kg}^{-1}$ ) at sea level presented in Ref. 79 for isotopes induced in  $\text{TeO}_2$  combining measured cross sections at different energies and in Ref. 81 for natural tellurium using ACTIVIA and TENDL library. Different cosmic neutron spectra were considered in the two works.

| Isotope            | Half-life <sup>68</sup> | Ref. 79              | Ref. 81 |
|--------------------|-------------------------|----------------------|---------|
| $^{110m}\text{Ag}$ | 249.78 d                | $4.9 \cdot 10^{-3}$  | 2.39    |
| $^{60}\text{Co}$   | 5.2711 y                | $<6.3 \cdot 10^{-5}$ | 0.81    |

in the background model of the CUORE experiment,<sup>80</sup> were combined with results from tellurium activation measurements with 800 MeV-23 GeV protons to estimate the corresponding production rates for CUORE crystals, considering the Gordon et al. spectrum. These results are reported in Table 4.

Within the SNO+ project, as described in Ref. 81, production rates of cosmogenic-induced isotopes on a natural tellurium target were calculated using the ACTIVIA program for energies above 100 MeV, the neutron and proton cross sections from TENDL library in the 10-200 MeV range when available, and the cosmogenic neutron and proton flux parametrization at sea level from Armstrong<sup>39</sup> and Gehrels.<sup>40</sup> An extensive set of isotopes was considered and even expected activation underground was evaluated too. Some results are shown in Table 4. Although not directly comparable with the estimated rates in Ref. 79 for the different targets, there is an important discrepancy between them. As shown in the excitation functions plotted in Ref. 81 for  $^{110m}\text{Ag}$  and  $^{60}\text{Co}$ , the measured cross sections above 800 MeV agree reasonably well with predictions of ACTIVIA; the origin of the difference can be at lower energies (the region giving the dominant contribution to the production rates). The different cosmic neutron spectra considered in the two works makes difficult also the comparison.

## 6. Sodium Iodide

Sodium iodide is being used for dark matter searches for a long time and in the last years activation yields in these crystals have started to be quantified in the context of various experiments. The observation of the annual modulation signal registered in the data of the DAMA/LIBRA experiment<sup>82</sup> for many years is the goal of projects at different stages of development like KIMS<sup>83</sup> and DM-Ice<sup>84</sup> (now joint in COSINE), ANAIS,<sup>85</sup> SABRE,<sup>86</sup> PICO-LON<sup>87</sup> and COSINUS.<sup>88</sup>

A first direct estimate of production rates of several iodine, tellurium and sodium isotopes induced in NaI(Tl) crystals was presented in Ref. 89. The estimate, developed in the frame of the dark matter ANAIS experiment, was based on data from two 12.5 kg NaI(Tl) detectors produced by Alpha Spectra Inc. which were installed inside a convenient shielding at the Canfranc Underground Laboratory at the end of 2012, just after finishing surface exposure to cosmic rays during production. The

Table 5. Production rates (in  $\text{kg}^{-1}\text{d}^{-1}$ ) at sea level for isotopes induced in NaI(Tl) crystals following measurements by ANAIS<sup>89</sup> and DM-Ice17<sup>90</sup> experiments together with calculations based on selected excitation functions<sup>89</sup> or using the ACTIVIA code.<sup>90</sup>

| Isotope            | Half-life <sup>67,68</sup> | Calculation <sup>89</sup> | Measurement <sup>89</sup> | ACTIVIA <sup>90</sup> | Measurement <sup>90</sup> |
|--------------------|----------------------------|---------------------------|---------------------------|-----------------------|---------------------------|
| <sup>126</sup> I   | 12.93 d                    | 297.0                     | 283±36                    | 128                   |                           |
| <sup>125</sup> I   | 59.407 d                   | 242.3                     | 220±10                    | 221                   | 230                       |
| <sup>127m</sup> Te | 107 d                      | 7.1                       | 10.2±0.4                  | 93                    | <9                        |
| <sup>125m</sup> Te | 57.4 d                     | 41.9                      | 28.2±1.3                  | 74                    | 27                        |
| <sup>123m</sup> Te | 119.3 d                    | 33.2                      | 31.6±1.1                  | 52                    | 21                        |
| <sup>121m</sup> Te | 154 d                      | 23.8                      | 23.5±0.8                  | 93                    | 25                        |
| <sup>121</sup> Te  | 19.16 d                    | 8.4                       | 9.9±3.7                   | 93                    |                           |
| <sup>113</sup> Sn  | 115.09 d                   |                           |                           | 9.0                   | 16                        |
| <sup>22</sup> Na   | 2.6029 y                   | 53.6                      | 45.1±1.9                  | 66                    |                           |

very fast start of data taking allowed to identify and quantify isotopes with half-lives of the order of tens of days. Initial activities underground were measured following the evolution of the identifying signatures for each isotope along several months; then, production rates at sea level were properly estimated according to the history of detectors. Production rates were also computed for comparison using the cosmic neutron flux at sea level from Gordon et al. and a description of excitation functions, carefully selected minimizing deviation factors between measured cross sections and calculations from MENDL2N, TENDL-2013, YIELDX and HEAD-2009. The ratio between calculated and measured production rates ranges from 0.7 to 1.5 for the observed isotopes. The obtained rates are reported in Table 5.

A complete study of cosmogenic activation in NaI(Tl) crystals was also performed within the DM-Ice17 experiment.<sup>90</sup> Two crystals, with a mass of 8.5 kg each and previously operated at the dark matter NaIAD experiment in the Boulby underground laboratory in UK,<sup>91</sup> were deployed at a depth of 2450 m under the ice at the geographic South Pole in December 2010 and collected data over three-and-a-half years. The activation of detector components occurred during construction, transportation, or storage at the South Pole prior to deployment. The DM-Ice17 data provided compelling evidence of significant production of cosmogenic isotopes, which was used to derive the corresponding production rates based on simulation matching. In addition, calculations based on modified ACTIVIA using the Gordon et al. neutron spectrum were also carried out. Results are presented in Table 5. A very good agreement between measured production rates in ANAIS and DM-Ice17 crystals has been found. ACTIVIA estimates of metastable tellurium isotopes give rates clearly higher than measured values.

Presence of cosmogenic isotopes has been also observed in NaI(Tl) crystals from other experiments.<sup>83,92-94</sup> In particular, in Ref. 92, the fraction of <sup>129</sup>I (which can be produced by uranium spontaneous fission and by cosmic rays) in DAMA/LIBRA crystals from Saint Gobain company was determined to be  $^{129}\text{I}/^{nat}\text{I} = (1.7 \pm 0.1) \times 10^{-13}$ ; strong variability of this concentration is expected in different origin ores.

The tritium content in NaI(Tl) detectors devoted to dark matter searches could

be very relevant. The tritium activity in DAMA/LIBRA crystals was constrained to be  $<0.09$  mBq/kg (95% C.L.).<sup>92</sup> A direct identification of tritium in NaI(Tl) crystals has not been possible, but within the ANAIS experiment, the construction of a detailed background model of the operated modules in the Canfranc Underground Laboratory (based on a Geant4 simulation of quantified background components) points to the need of an additional background source contributing only in the very low energy region, which could be tritium.<sup>95</sup> The inclusion of a certain activity of  $^3\text{H}$  homogeneously distributed in the NaI crystal provides a very good agreement between measured data and the model below 20 keV. For two Alpha Spectra detectors, both fabricated in Alpha Spectra facilities at Grand Junction, Colorado (where the cosmic neutron flux is estimated to be a factor  $f = 3.6$  times higher than at sea level<sup>89</sup>) but with different production history, the required  $^3\text{H}$  initial activities (that is, at the moment of going underground) to reproduce the data are around 0.20 mBq/kg and 0.09 mBq/kg; the latter value is just the upper limit set for DAMA/LIBRA crystals. These results boosted the study of tritium production in NaI.

Only calculations of the tritium production rate are available; results using TALYS,<sup>59</sup> GEANT4<sup>37</sup> and ACTIVIA<sup>37,90</sup> are shown in Table 3. In the calculations of Ref. 71, based on a selection of excitation functions mainly from TENDL for neutrons and HEAD-2009 libraries, there is a significant difference in the medium energy range between the two estimates of cross sections for I, being those from TENDL much higher; this fact is responsible of the large uncertainty in the production rate estimated for NaI. As it can be seen in Table 3, this rate is higher than previous estimates, but the required exposure times to get the deduced tritium activities for ANAIS detectors based on that rate roughly agree with the time lapse between sodium iodide raw material purification starting and detector shipment, according to the company.<sup>71</sup>

## 7. Xenon

Xenon-based detectors are being extensively used in the investigation of rare events. Following very successful predecessors, many efforts are now concentrated in the XENON1T,<sup>96</sup> LUX-ZEPLIN,<sup>97</sup> PANDAX<sup>98</sup> or XMASS<sup>99</sup> projects in the search for dark matter; EXO,<sup>100</sup> KamLAND-Zen<sup>101</sup> and NEXT<sup>102</sup> are looking for the neutrinoless double beta decay of  $^{136}\text{Xe}$ . Even if in liquid xenon experiments, the purification system is presumed to suppress the concentration of non-noble radioisotopes below significance, there are several estimates of production rates of activated isotopes in xenon based on both direct measurements and calculations following different approaches. As it will be shown, the dispersion in results for most of the analyzed products in this material is important. Production of xenon radioisotopes could be problematic due to low energy deposits, which can be a relevant background in the WIMP search energy region; but these backgrounds soon reach negligible levels once xenon is moved underground.<sup>97</sup>

A first dedicated study on the cosmogenic activation of xenon was presented in Ref. 103, complemented by a study of copper activated simultaneously. Samples were exposed to cosmic rays in a controlled manner at the Jungfraujoch research station (at 3470 m above sea level in Switzerland) for 345 days. The xenon sample, with a mass of  $\sim 2$  kg, had natural isotopic composition. The samples were screened with a low-background germanium detector (named Gator) in the Gran Sasso underground laboratory before and after activation to quantify the cosmogenic products. Saturation activities were derived for several long-lived isotopes and some results are shown in Table 6. The measured results were compared in addition to predictions using ACTIVIA and COSMO packages, including the neutron spectrum from Refs. 39, 40. It is worth noting that from all the directly observed radionuclides, only  $^{125}\text{Sb}$  is considered to be a potential relevant background for a multi-ton scale dark matter search.

For natural xenon, production rates of several isotopes were estimated as made for germanium in Ref. 59, with excitation functions calculated using TALYS code, and as for different materials in Ref. 37, from GEANT4 simulation or ACTIVIA calculations. For GEANT4 simulations, the set of electromagnetic and hadronic physics processes included in the Shielding modular physics list were taken into account while in ACTIVIA, cross sections are obtained from data tables and semiempirical formulae. It is worth noting that in the results shown here the Gordon et al. neutron spectrum was considered for both GEANT4 and ACTIVIA, which required a modification of the latter. Some of these results are also shown in Table 6. In these calculations, the production rate of  $^3\text{H}$  was also evaluated and it is presented in Table 3.

The analysis of the radiogenic and muon-induced backgrounds in the LUX dark matter detector operating at the Sanford Underground Research Facility in US allowed to quantify the cosmogenic production of some xenon radioisotopes.<sup>104</sup> In particular, zero-field data taken 12 days after the xenon was moved underground and 70 days before the start of the WIMP search run were considered. Some of the obtained saturation activities, as reproduced in Ref. 103, are presented in Table 6.

In the context of neutrinoless double beta decay experiments working with xenon enriched in  $^{136}\text{Xe}$ , the production of short-lived  $^{137}\text{Xe}$  by neutron capture can be relevant and is considered as a background source. This isotope is the only cosmogenic radionuclide found to have a significant contribution in their region of interest;<sup>105</sup> the measured capture rate by the EXO-200 experiment is  $338^{+132}_{-93}$  captures on  $^{136}\text{Xe}$  per year. In addition, individual production cross sections for 271 radionuclides have been determined for  $^{136}\text{Xe}$  in an inverse kinematics experiment at GSI.<sup>106</sup>

## 8. Argon

Different projects use liquid argon in dark matter detectors, like ArDM,<sup>107</sup> DarkSide<sup>108</sup> or DEAP/CLEAN,<sup>109</sup> and also gaseous argon is considered in the TREX-DM experiment.<sup>110</sup> The most worrisome background source in this detector medium



Table 6. Production rates or saturation activities (in  $\mu\text{Bq kg}^{-1}$ ) at sea level for isotopes induced in natural xenon following measurements in Refs. 103,104 and different calculations based on COSMO, ACTIVIA (considering different cosmic neutron spectra), TALYS and GEANT4.

|                             | $^7\text{Be}$       | $^{101}\text{Rh}$    | $^{125}\text{Sb}$   | $^{121m}\text{Te}$ | $^{123m}\text{Te}$ | $^{127}\text{Xe}$    |
|-----------------------------|---------------------|----------------------|---------------------|--------------------|--------------------|----------------------|
| Half-life <sup>67, 68</sup> | 53.22 d             | 3.3 y                | 2.759 y             | 154 d              | 119.3 d            | 36.358 d             |
| Measurement <sup>103</sup>  | $370^{+240}_{-230}$ | $1420^{+970}_{-850}$ | $590^{+260}_{-230}$ | <1200              | <610               | $1870^{+290}_{-270}$ |
| Measurement <sup>104</sup>  |                     |                      |                     |                    |                    | $1530\pm 300$        |
| COSMO <sup>103</sup>        | 6.4                 | 15.3                 | 13.5                | 276                | 14.4               | 555                  |
| ACTIVIA <sup>103</sup>      | 6.4                 | 16.6                 | 0.2                 | 299                | 14.7               | 415                  |
| ACTIVIA <sup>37</sup>       |                     |                      | 0.10                | 630.3              | 30.9               | 1041.0               |
| GEANT4 <sup>37</sup>        |                     |                      | 17.1                | 245.4              | 213.8              | 2700.2               |
| TALYS <sup>59</sup>         |                     | 0.46                 | 0.46                | 135.4              | 140.0              |                      |

is  $^{39}\text{Ar}$ , a  $\beta^-$  emitter with an endpoint energy of 565 keV and half-life of 269 y.<sup>67</sup>  $^{39}\text{Ar}$  is present in atmospheric argon as it is mainly produced by cosmic ray induced nuclear reactions such as  $^{40}\text{Ar}(n,2n)^{39}\text{Ar}$ . In the context of the WARP experiment at the Laboratori Nazionali del Gran Sasso (LNGS),  $^{39}\text{Ar}$  activity in natural argon was measured to be at the level of 1 Bq/kg.<sup>111</sup> But the discovery of argon from deep underground sources with significantly less  $^{39}\text{Ar}$  content has allowed to improve the background prospects of experiments using argon as the active target. In Ref. 112, a specific  $^{39}\text{Ar}$  activity of less than 0.65% of the activity in atmospheric argon corresponding to 6.6 mBq/kg was measured for underground argon from a  $\text{CO}_2$  plant in Colorado; results from the DarkSide experiment have shown that the underground argon contains  $^{39}\text{Ar}$  at a level reduced by a factor  $(1.4\pm 0.2)\times 10^3$  relative to atmospheric one.<sup>108</sup>

Concerning the tritium production in argon (or neon, which is in some cases considered as an alternative target), there is no experimental information. As shown in Table 3, there are some estimates of the production rate in argon using TALYS code<sup>59</sup> and GEANT4 and ACTIVIA (using the Gordon et al. neutron spectrum).<sup>37</sup> Since there was no information for neon, in Ref. 71, the study of tritium production performed for other targets like germanium and sodium iodide was applied also to argon and neon, selecting the excitation functions and considering the Gordon et al. cosmic neutron spectrum. If saturation activity was reached for tritium, according to the production rates deduced in this study and presented in Table 3 too, tritium could be very problematic. However, tritium is expected to be suppressed by purification of gas and minimizing exposure to cosmic rays of the purified gas should avoid any problematic tritium activation.

## 9. Copper

Copper is a material widely used in rare event experiments due to its mechanical, thermal and electrical properties, either as shield or part of the detector components. Copper is also a specially interesting material for activation studies because

there are many extensive sets of measurements of production cross sections for protons and even for neutrons; this makes it very attractive to compare calculations and experimental data in order to allow a good validation of excitation functions. The most relevant results on the quantification of activation yields in copper are presented in this section.

- As for germanium, the ACTIVIA code, including the energy spectrum for cosmic ray neutrons at sea level from Refs. 39,40, was used to evaluate production rates in copper for benchmark.<sup>17</sup>
- Direct measurements of production rates were made in LNGS.<sup>113</sup> Seven plates made of NOSV grade copper from Nord-deutsche Affinerie AG (Germany), with a total weight of 125 kg, were exposed for 270 days at an outside hall of the LNGS (altitude 985 m) under a roof. Screening with one GeMPI detector was carried out for 103 days. Production rates were derived as the measured saturation activity. The highest values were found for cobalt isotopes; in particular, the measured activity of <sup>60</sup>Co ((2100±190) μBq/kg) greatly exceeded the upper limit derived for the primordial activity. The production rates at sea level are reproduced in Table 7, including a correction factor estimated to be 2.1 (following Ref. 41) due to the altitude during exposure.
- The same study of evaluation of excitation functions based of deviation factors and estimate of production rates made for germanium was also carried out for copper in Ref. 61. Production rates were calculated using below 100 MeV MENDL2N results for neutrons normalized to the available experimental data if possible, and above that energy experimental data for protons combined with YIELDX calculations when necessary. Differences in the production rates estimated in this work due to the different neutron spectra considered are similar to those obtained in germanium: production rates considering the Ziegler parametrization are higher than the corresponding ones using the expression from Gordon et al. Results shown in Table 7 are the ones obtained using the Gordon spectrum.
- Together with the dedicated study on the cosmogenic activation of xenon, a study on copper was simultaneously carried out in Ref. 103. Samples were exposed to cosmic rays in a controlled manner at the Jungfraujoch research station (at 3470 m above sea level in Switzerland) for 345 days. The 10.35 kg copper sample consisted of 5 blocks of OFHC copper from Norddeutsche Affinerie (now Aurubis), from the batch used to construct inner parts of the XENON100 detector. Before each measurement, copper was properly cleaned to remove surface contaminations. The samples were screened with the Gator low-background germanium detector in the Gran Sasso underground laboratory before and after activation to quantify the cosmogenic products. Saturation activities were derived and some results are presented in Table 7. The measured results were compared in addition to predictions using ACTIVIA and COSMO packages, including the neutron spectrum from Refs. 39,40.
- As for different materials, production rates of several isotopes were estimated in

Table 7. Production rates (in  $\text{kg}^{-1} \text{d}^{-1}$ ) at sea level for isotopes induced in natural copper following measurements in Refs. 103, 113 and different calculations (see text).

|                                  | $^{46}\text{Sc}$       | $^{48}\text{V}$     | $^{54}\text{Mn}$     | $^{59}\text{Fe}$    | $^{56}\text{Co}$    | $^{57}\text{Co}$     | $^{58}\text{Co}$     | $^{60}\text{Co}$     |
|----------------------------------|------------------------|---------------------|----------------------|---------------------|---------------------|----------------------|----------------------|----------------------|
| Half-life <sup>67,68</sup>       | 83.787 d               | 15.9735 d           | 312.19 d             | 44.494 d            | 77.236 d            | 271.82 d             | 70.85 d              | 5.2711 y             |
| Measurement <sup>113</sup>       | $2.18 \pm 0.74$        | $4.5 \pm 1.6$       | $8.85 \pm 0.86$      | $18.7 \pm 4.9$      | $9.5 \pm 1.2$       | $74 \pm 17$          | $67.9 \pm 3.7$       | $86.4 \pm 7.8$       |
| Measurement <sup>103</sup>       | $2.33^{+0.95}_{-0.78}$ | $3.4^{+1.6}_{-1.3}$ | $13.3^{+3.0}_{-2.9}$ | $4.1^{+1.4}_{-1.2}$ | $9.3^{+1.2}_{-1.4}$ | $44.8^{+8.6}_{-8.2}$ | $68.9^{+5.4}_{-5.0}$ | $29.4^{+7.1}_{-5.9}$ |
| ACTIVIA <sup>17,103</sup>        | 3.1                    |                     | 14.3                 | 4.2                 | 8.7                 | 32.5                 | 56.6                 | 26.3                 |
| ACTIVIA (MENDL-2P) <sup>17</sup> | 3.1                    |                     | 12.4                 | 1.8                 | 14.1                | 36.4                 | 38.1                 | 9.7                  |
| TALYS <sup>59</sup>              |                        |                     | 16.2                 |                     |                     | 56.2                 |                      | 46.4                 |
| MENDL+YIELDX <sup>61</sup>       | 2.7                    |                     | 27.7                 | 4.9                 | 20.0                | 74.1                 | 123.0                | 55.4                 |
| COSMO <sup>103</sup>             | 1.5                    | 3.1                 | 13.5                 | 4.3                 | 7.0                 | 30.2                 | 54.6                 | 25.7                 |
| GEANT4 <sup>37</sup>             | 1.2                    |                     | 12.3                 | 8.8                 | 10.3                | 67.2                 | 57.3                 | 64.6                 |
| ACTIVIA <sup>37</sup>            | 4.1                    |                     | 30.0                 | 10.5                | 20.1                | 77.5                 | 138.1                | 66.1                 |

Ref. 59 using TALYS and in Ref. 37 from GEANT4 simulation or ACTIVIA calculations, considering the Gordon et al. parametrization for the neutron spectrum. Some of these results are also shown in Table 7.

- In Ref. 114, the cosmogenic activity produced in copper to be used as radiation shielding was measured, using a HPGe detector operated in the Canfranc Underground Laboratory. A sample with a mass of 18 kg, exposed at 250 m above sea level for 1 year after casting according to company records, as well as bricks exposed to cosmic rays for 41 days, were analyzed. Activities found for cobalt isotopes and  $^{54}\text{Mn}$  agree with the expectations from previously measured production rates.

Comparing all the information on production rates on copper available and summarized in Table 7, it can be seen that measured rates from the two independent activation experiments are in very good agreement for some isotopes, but there are differences for others, specially for  $^{60}\text{Co}$ . In general, higher rates were found in Ref. 113. The different calculations give results with important dispersion; it must be noted that ACTIVIA calculations reported in Table 7 were obtained using different descriptions of the cosmic neutron spectrum.

## 10. Lead

Even if tons of lead are commonly used in rare event experiments as radiation shielding, activation studies on this material are scarce. In Ref. 115, results for some production rates are presented following the irradiation of a natural lead sample at LANSCE using the neutron beam resembling the cosmic neutron flux and after counting the amount of radioactive isotopes using a low background, underground germanium detector at WIPP. By scaling the LANSCE neutron flux to a cosmic neutron flux, the sea level production rates of some long-lived radionuclides were estimated and are reported in Table 8; calculations based on TALYS code and the Gordon et al. neutron spectrum deduced in the same work are also shown. In Ref. 115 it is concluded that for ordinary exposures, the cosmogenic background is

Table 8. Production rates (in  $\text{kg}^{-1}\text{d}^{-1}$ ) at sea level for isotopes induced in natural lead following an irradiation experiment at LANSCE and TALYS calculations.

| Isotope           | Half-life (y) <sup>67,68</sup> | Measurement <sup>115</sup> | TALYS <sup>115</sup> |
|-------------------|--------------------------------|----------------------------|----------------------|
| <sup>194</sup> Hg | 444                            | $8.0\pm 1.3$               | 16                   |
| <sup>202</sup> Pb | $5.25 \cdot 10^4$              | $120\pm 25$                | 77                   |
| <sup>207</sup> Bi | 32.9                           | $<0.17$                    |                      |

Table 9. Production rates (in  $\text{kg}^{-1}\text{d}^{-1}$ ) at sea level for isotopes induced in stainless steel, from the measurement following an exposure to cosmic rays in Gran Sasso and from calculations using GEANT4 and ACTIVIA packages.

| Isotope          | Half-life (d), <sup>67,68</sup> | Measurement <sup>113</sup> | GEANT4 <sup>37</sup> | ACTIVIA <sup>37</sup> |
|------------------|---------------------------------|----------------------------|----------------------|-----------------------|
| <sup>7</sup> Be  | 53.22                           | $389\pm 60$                | 0.05                 | 2.05                  |
| <sup>54</sup> Mn | 312.19                          | $233\pm 26$                | 230                  | 191                   |
| <sup>58</sup> Co | 70.85                           | $51.8\pm 7.8$              | 90                   | 13                    |
| <sup>56</sup> Co | 77.236                          | $20.7\pm 3.5$              | 16                   | 131                   |
| <sup>46</sup> Sc | 83.787                          | $19.0\pm 3.5$              | 8.8                  | 18                    |
| <sup>48</sup> V  | 15.9735                         | $34.6\pm 3.5$              |                      |                       |

less than that from the naturally occurring radioisotopes in lead.

## 11. Stainless Steel

Stainless steel is also very often used in experiments and some activation studies are available. Direct measurements of saturation activity were made in LNGS.<sup>113</sup> Samples of stainless steel (1.4571 grade) from different batches supplied by Nironit company (with masses from 53 to 61 kg) were screened with GeMPI detector at Gran Sasso for the GERDA double beta decay experiment.<sup>116</sup> One of these samples was re-exposed for 314 days in open air at the LNGS outside laboratory, after a cooling time of 327 days underground. Production rates were derived for Gran Sasso altitude and scaled down to sea level, considering a correction factor of 2.4. In this case, <sup>60</sup>Co is obscured by anthropogenic contamination, generally present in steel. The obtained results are reported in Table 9.

In Ref. 37, calculations of production rates for stainless steel have been performed using GEANT4 and ACTIVIA and are also shown in Table 9. Comparing measured and calculated rates, agreement is better in some products for ACTIVIA and in others for GEANT4. None of the codes predicts the important activation yield measured for <sup>7</sup>Be.

## 12. Titanium

Titanium has been considered due to its properties as an alternative to stainless steel and copper. Indeed, a reduced cosmogenic activation is expected in this material. In the frame of the LUX experiment, radiopurity of different titanium samples

Table 10. Production rates (in  $\text{kg}^{-1}\text{d}^{-1}$ ) at sea level for some isotopes induced in titanium from calculations using GEANT4 and ACTIVIA packages.

|                  | Half-life <sup>68</sup> | GEANT4 <sup>37</sup> | ACTIVIA <sup>37</sup> |
|------------------|-------------------------|----------------------|-----------------------|
| <sup>46</sup> Sc | 83.787 d                | 275.5                | 270.1                 |
| <sup>40</sup> K  | 1.25 10 <sup>9</sup> y  | 22.1                 | 61.0                  |

was analyzed<sup>117,118</sup> and the activity of cosmogenic <sup>46</sup>Sc was quantified, ranging from 0.2 to 23 mBq/kg. Other scandium isotopes with shorter half-lives were also observed but are not relevant. One 6.7 kg control titanium sample was used to directly estimate the cosmogenic yields; the sample was screened at the Soudan Low Background Counting Facility (SOLO) after two years underground and then transported by ground to the Sanford Surface Laboratory in South Dakota. The sample was activated over a six-month period before being transported by ground back to SOLO for re-analysis. The measured activity was  $(4.4 \pm 0.3)$  mBq/kg of <sup>46</sup>Sc,<sup>104</sup> which agrees within a factor two with the expected result following the calculations in Ref. 37. In this work, production rates of <sup>46</sup>Sc and other isotopes were estimated using GEANT4 and ACTIVIA, as shown in Table 10.

### 13. Other Results

Here, some results related to the observation and analysis of cosmogenic activation for other materials are briefly reported.

Cosmogenic activation was found to play an important role in the scintillating **CaWO<sub>4</sub>** crystals operated as cryogenic detectors in the CRESST-II dark matter experiment, following the extensive background studies of a crystal (called TUM40), grown at the Technische Universitat Munchen.<sup>119</sup> Distinct gamma lines were observed in the low-energy spectrum below 80 keV, originating from activation of W isotopes: proton capture on <sup>182</sup>W and <sup>183</sup>W results in <sup>179</sup>Ta (after a successive decay) and <sup>181</sup>W respectively, which decay via electron capture. The activity of both isotopes in the crystal was quantified and, as the leaking of events from this background source into the region of interest for dark matter searches is very important, initiatives to reduce the cosmogenic activation of crystals have been undertaken. On the other hand, the production rate of tritium in CaWO<sub>4</sub> was evaluated using the TALYS code<sup>59</sup> and it is reported in Table 3. Radioactive contamination, including some cosmogenic products, measured for different inorganic crystal scintillators like CaWO<sub>4</sub> is presented in Ref. 120.

Excitation functions of proton-induced reactions on natural **neodymium**, in the 10-30 MeV energy range, were measured in Ref. 121. Irradiation took place at the cyclotron U-120M in Rez near Prague and the radioactivity measurement was carried out using a HPGe detector. The measured production cross sections were compared with TENDL-2010 predictions finding in general good agreement in both

shapes and absolute values. In addition, the corresponding contribution to the production rates of radionuclides relevant for double beta decay searches, like in the SNO+ experiment, was evaluated adopting the proton flux from Ref. 35. In Ref. 122, these results were completed in 5-35 MeV energy range following an analogue experimental strategy and comparing with excitation functions from TENDL-2012 library.

The same experiment performed for tellurium and germanium was also made with a natural **molybdenum** target, based on 800 MeV proton irradiation at LAN-SCE and screening with germanium detectors at Berkeley,<sup>58</sup> for determining the <sup>60</sup>Co production cross section.

In Ref. 37, the production rates of a few isotopes (<sup>7</sup>Be, <sup>10</sup>Be and <sup>14</sup>C) induced in **PTFE** are presented, based on analogous calculations to those performed for xenon, copper, titanium and stainless steel using GEANT4 and ACTIVIA.

For **quartz** light guides, some production rates were calculated in Ref. 90 using ACTIVIA with the Gordon et al. neutron spectrum, including that of tritium reproduced in Table 3.

#### 14. Underground Activation

At a depth of a few tens of meter water equivalent (m.w.e.), the nucleonic component of the cosmic flux is reduced to a negligible level. The neutron fluxes in underground facilities, either radiogenic (from fission or ( $\alpha$ ,n) reactions) or induced by cosmic muons, in rock or set-up materials, are several orders of magnitude lower than at surface. The spectrum of the dominant component is concentrated at the region of a few MeV, which is below the energy threshold of most of the spallation processes activating materials at surface. In addition, to suppress the neutron activation underground it could be possible to use a neutron moderator shielding around the detector. Therefore, the cosmogenic production underground is often assumed to be negligible. The considered generation of radioactive isotopes underground is induced mainly by muons. At shallow depths, the capture of negative muons is the relevant process but deep underground interactions by fast muons dominate (direct muon spallation or the electromagnetic and nuclear reactions induced by secondary particles: nucleons, pions, photons, . . .). Since the muon flux and spectrum depends on depth, it is worth noting that underground activation studies are produced for particular depths; therefore, comparison of different estimates is not straightforward.

Many of the results obtained for underground activation are related with experiments using large liquid scintillator detectors, as summarized in the following.

- An early estimate of production rates was made in Ref. 123 for isotopes induced in materials typically used in neutrino experiments: C, O and Ar. Inelastic scattering of muons giving electromagnetic nuclear reactions was considered and rates were evaluated at sea level and underground (2700 m.w.e.).
- Production cross sections were measured in a reference experiment<sup>124</sup> performed

at CERN irradiating with the SPS muon beam with energies of 100 and 190 GeV different kinds of  $^{12}\text{C}$  targets placed behind concrete and water to build the muon shower like in real liquid scintillator experiments. Several detection techniques for measuring products of different half-lives were applied. Then, considering the measured cross-sections and the deduced dependence with the muon energy ( $\sigma \propto E_\mu^\alpha$  with  $\alpha = 0.73 \pm 0.10$ ) muon induced background rates for the muon flux at Gran Sasso and BOREXINO detector were computed.<sup>124</sup> Rates for KamLAND were estimated to be a factor  $\sim 7$  higher. The most relevant contribution was that of  $^{11}\text{C}$ .

- In fact, the production rate of  $^{11}\text{C}$  was specifically estimated in Ref. 125 taking into account all relevant production channels. Evaluation of cross sections from different sources combining data and calculations was made and a FLUKA simulation of monoenergetic muons in Borexino liquid scintillator (trimethylbenzene) was run to derive rates and paths of secondary particles; then, combining this information on the secondaries with the cross sections the individual and total production rates were derived for different muon energies. Good agreement was found with rates coming from measurements (at 100 and 190 GeV)<sup>124</sup> and with extrapolations for average muon energies at KamLAND, Borexino and SNOlab.
- Analysis of KamLAND data (from 2002 to 2007) allowed the measurement of activation yields.<sup>126</sup> Isotopes were identified and quantified using energy and time information registered. In addition, a FLUKA simulation of monoenergetic muons (in the 10 to 350 GeV range) was performed for KamLAND liquid scintillator to estimate the same yields too. Comparing with extrapolations (based on the power-law dependance with respect to muon energy) of results from the muon beam experiment,<sup>124</sup> some inconsistencies are reported for some isotopes, indicating that estimation by extrapolation might not be sufficient.
- In Ref. 127, from data from the Borexino experiment and profiting the large sample of cosmic muons identified and tracked by a muon veto external to the liquid scintillator, not only the yield of muon-induced neutrons was characterized but also the production rates of a number of cosmogenic radioisotopes ( $^{12}\text{N}$ ,  $^{12}\text{B}$ ,  $^8\text{He}$ ,  $^9\text{C}$ ,  $^9\text{Li}$ ,  $^8\text{B}$ ,  $^6\text{He}$ ,  $^8\text{Li}$ ,  $^{11}\text{Be}$ ,  $^{10}\text{C}$  and  $^{11}\text{C}$ ) were measured, based on a simultaneous fit to energy and decay time distributions. Results of the corresponding analysis performed by the KamLAND collaboration for the Kamioka underground laboratory are similar. All results are compared with Monte Carlo simulation predictions using the FLUKA and Geant4 packages. General agreement between data and simulation is observed within their uncertainties with a few exceptions; the most prominent case is  $^{11}\text{C}$  yield, for which both codes return about 50% lower values.
- In the context of argon-based neutrino experiments, production of  $^{40}\text{Cl}$  and other cosmogenically produced nuclei (isotopes of P, S, Cl, Ar and K) which can be potential sources of background was evaluated in Ref. 128.  $^{40}\text{Cl}$  can be produced through stopped muon capture and the muon-induced neutrons and protons via (n,p) and (p,n) reactions; it is unwanted as it can be a background for different neutrino reactions. Geant4 simulations were carried out and analytic models were

developed, using the measured muon fluxes at different levels of the Homestake Mine. Different depths were considered in the study, concluding that large backgrounds to the physics proposed are expected at a depth of less than 4 km.w.e.

Studies of underground activation have been made too in other contexts, not related to large scintillator detectors.

- Estimates of production rates for isotopes produced in enriched germanium detectors and set-up materials (cryogenic liquid) were made within the GERDA double beta decay experiment,<sup>129</sup> based on a GEANT4 Monte Carlo simulation for the muon spectrum at Gran Sasso.  $^{77m}\text{Ge}$  was identified as the most relevant product.
- In Ref. 130, the radioactivity induced by cosmic rays, including neutrinos, muons and neutrons, is analyzed for the rock salt cavern of an underground laboratory. Natural isotopes of sodium and chlorine are considered.
- The activation in natural tellurium due to the neutron flux underground, in particular for Sudbury laboratory (at a depth of about 6 km.w.e.), was analyzed in Ref. 81. For long-lived isotopes, the underground activation was estimated to be less than 1 event/(y t). The production rates for many short-lived isotopes of Sn, Sb and Te were quantified using ACTIVIA and TENLD data, for neutrons coming from ( $\alpha$ ,n) reactions as well as for muon-induced neutrons; the obtained rates are many orders of magnitude lower than the derived rates following the same approach for exposure at surface.
- The production of  $^{127}\text{Xe}$  in xenon detectors at the depth of the Sanford Underground Research Facility (1480 m below surface, 4.3 km.w.e.) was evaluated in Ref. 37 by Geant4 simulation, considering contributions from both fast and thermal neutrons. A production rate of about 3 atoms per ton per day, considered to be negligible, was found.

## 15. Summary

Cosmogenic activation of materials can jeopardize the sensitivity of experiments demanding ultra-low background conditions due to the production of long-lived isotopes on the Earth's surface by nucleons and, in some cases, also due to the continuous generation of short-lived radionuclides deep underground by fast muons. With the continuous increase of detector sensitivity and reduction of primordial radioactivity of materials, this background source is becoming more and more relevant. Direct measurements and estimates of production rates and yields for several materials have been made in the context of, for instance, dark matter, double beta decay and neutrino experiments. As summarized here, cosmogenic products have been analyzed for materials used as detector media and also for common materials used in ancillary components. Each material produces different relevant cosmogenic isotopes, although there are some ones generated in most of the materials; this is the case of tritium, which due to its decay properties is specially relevant for dark



matter searches.

In principle, sea level activation can be kept under control by minimizing exposure at surface and applying material purification techniques. But reliable tools to quantify the real danger of exposing the materials to cosmic rays are desirable. There are many options to undertake a material activation study, but unfortunately, discrepancies between different estimates are usually non-negligible. At the moment, there is no approach working better than others for all targets and products. A good recipe to attempt the calculation of the production rate of a particular isotope could be the following:

- (1) To collect all the available information on its production cross section by neutrons and protons, from both measurements (EXFOR database will help) and calculations, either from libraries or using codes (based on semiempirical formulae like YIELDX and ACTIVIA or on Monte Carlo simulation). Measurements of cross sections at different energies using nucleon beams are not straightforward, but they are essential to validate models and codes giving excitation functions.
- (2) To choose the best description of the excitation functions of products over the whole energy range, by minimizing deviation factors between measurements and calculations.
- (3) To calculate the production rates considering the preferred cosmic ray spectrum and to compare them with previous estimates or measurements if available.

Uncertainties in this kind of calculations (in many cases higher than 50%) come mainly from the difficulties encountered both on the accurate description of cosmic ray spectra and on the precise evaluation of inclusive production cross-sections in all the relevant energy range; the low and medium energy regions below a few hundreds of MeV are the most problematic ones since neutron data are scarce and differences between neutron and proton cross sections may be important. Concerning the cosmic neutron spectrum at sea level, most of the activation studies performed in the last years have chosen the parametrization from Gordon et al.<sup>42</sup>

Presently, the experimental results for the production rates of cosmogenic radioisotopes are scarce and limited to a reduced number of materials, as they require precise knowledge of the exposure history of materials. But the availability in the future of more measured production rates either following dedicated measurements exposing samples to cosmic rays in a controlled environment or from the detailed analysis of background data collected within running experiments will help to achieve progress in the reduction of uncertainties when estimating activation yields in materials.

## References

1. G. Heusser, *Annu. Rev. Nucl. Part. Sci.* **45**, 543 (1995).
2. J. A. Formaggio and C. J. Martoff, *Annu. Rev. Nucl. Part. Sci.* **54**, 361 (2004).
3. P. Gondolo, *Nuclear Data Sheet* **120**, 175–179 (2014).

4. D. Lal and B. Peters, *Cosmic ray produced radioactivity on the Earth*, (Springer, Berlin-Heidelberg, 1967).
5. J. Beer, K. McCracken, R. von Steiger, *Cosmogenic Radionuclides. Theory and Applications in the Terrestrial and Space Environments*, (Springer, 2012).
6. S. Cebrián, *AIP Conf. Proc.* **1549**, 136–141 (2013).
7. V. Kudryavtsev, Presentation at Low Radioactivity Techniques 2017 workshop, Seoul, Korea, <http://indico.ibs.re.kr/event/46/session/7/contribution/20>.
8. Decay Data Evaluation Projet, [http://www.nucleide.org/DDEP\\_WG/Nuclides/H-3\\_tables.pdf](http://www.nucleide.org/DDEP_WG/Nuclides/H-3_tables.pdf).
9. <http://www.nndc.bnl.gov/exfor/exfor.htm>,  
<http://www-nds.iaea.org/exfor/exfor.htm>.
10. A. S. Iljinov et al., *Production of Radionuclides at Intermediate Energies*, (Springer-Verlag, Landolt-Börnstein series, subvolumes: I/13a (1991), I/13b (1992), I/13c (1993), I/13d (1994), I/13e (1994), I/13f (1995), I/13g (1996), I/13h (1996), I/13i (1999)).
11. R. Silberberg and C. H. Tsao, *Astrophys. J. Suppl. Ser.* **25**, 315 (1973); *ibid* p. 335.
12. R. Silberberg and C. H. Tsao, *Astrophys. J. Suppl. Ser.* **35**, 129 (1977).
13. R. Silberberg and C. H. Tsao, *Astrophys. J. Suppl. Ser.* **58**, 873 (1985).
14. R. Silberberg and C. H. Tsao, *Phys. Rep.* **191**, 351 (1990).
15. R. Silberberg and C. H. Tsao, *Astrophys. J.* **501**, 911 (1998).
16. C. J. Martoff and P. D. Lewin, *Comput. Phys. Commun.* **72**, 96 (1992).
17. J. J. Back and Y. A. Ramachers, *Nucl. Instrum. Meth. A* **586**, 286 (2008).
18. J. Allison et al., *Nucl. Instrum. Meth. A* **835**, 186–225 (2016).
19. T.T. Bhlen et al., *Nuclear Data Sheets*, **120**, 211–214 (2014).
20. <https://mcnp.lanl.gov/>.
21. E. Aguayo et al., *Phys. Rev. C* **90**, 034607 (2014).
22. Yu. A. Korovin et al., *Nucl. Instrum. Meth. A* **624**, 20–26 (2010).
23. Yu. A. Titarenko et al., *Phys. Rev. C* **84**, 064612 (2011).
24. <http://www-nds.iaea.org/public/rnal/www/>
25. A.J. Koning et al., *Neutron and Proton Transmutation-Activation Cross Section Libraries to 150 MeV for Application in Accelerator-Driven Systems and Radioactive Ion Beam Target-Design Studies*, ECN Report ECN-R-98-012, (Petten, The Netherlands, 1998).
26. <http://www-nds.iaea.org/publications/iaea-nds/iaea-nds-0136.htm>,  
<http://www.oecd-nea.org/tools/abstract/detail/iaea1376>.
27. A. J. Koning and D. Rochman, *Nuclear Data Sheets* **113**, 2841 (2012).
28. K. A. Van Riper, S. G. Mashnik and W. B. Wilson, *Nucl. Instrum. Meth. A* **463**, 576–585 (2001).
29. L.M. Oranj et al., *Nucl. Instr. and Meth. A* **677**, 22–24 (2012).
30. J. Vrzalova et al., *Nucl. Instr. and Meth. A* **726**, 84–90 (2013).
31. M. Zaman et al., *Eur. Phys. J. A* **51**, 104 (2015).
32. H. Azizakram et al., *App. Rad. Isot.* **112**, 147–155 (2016).
33. R. Baldik and A. Dombayci, *App. Rad. Isot.* **113**, 10–17 (2016).
34. M. Bhike et al., *Phys. Rev. C* **95**, 054605 (2017).
35. I. Barabanov et al., *Nucl. Instrum. Meth. B* **251**, 115–120 (2006).
36. W.Z. Wei et al., *Cosmogenic Activation of Germanium Used for Tonne-Scale Rare Event Search Experiments*, arXiv:1706.05324v1 [nucl-ex].
37. C. Zhang et al., *Astropart. Phys.* **84**, 62–69 (2016).
38. W. N. Hess, H. W. Patterson and R. Wallace, *Phys. Rev.* **116**, 449 (1959).
39. T.W. Armstrong, K.C. Chandler, J. Barish, *J. Geophys. Res.* **78**, 2715 (1973).

40. N. Gehrels, *Nucl. Instr. and Meth. A* **239**, 324 (1985).
41. J. F. Ziegler, *IBM J. Res. Develop.* **42**, 117–140 (1998).
42. M. S. Gordon et al., *IEEE Transactions on Nuclear Science* **51**, 3427 (2004). Erratum: M. S. Gordon et al., *IEEE Transactions on Nuclear Science* **52**, 2703 (2005).
43. Soft-error Testing Resources website, <http://seutest.com/cgi-bin/FluxCalculator.cgi>.
44. C. Hagmann et al., *IEEE Nuclear Science Symposium Conference Record V2*, 1143–1146 (2007).
45. C. Hagmann et al., Monte Carlo Simulation of Proton-induced Cosmic-ray Cascades in the Atmosphere, UCRL-TM-229452, [https://nuclear.llnl.gov/simulation/doc\\_cry\\_v1.7/cry\\_physics.pdf](https://nuclear.llnl.gov/simulation/doc_cry_v1.7/cry_physics.pdf)
46. A. Morales et al., *Phys. Lett. B* **532**, 8–14 (2002).
47. H.V. Klapdor-Kleingrothaus and I.V. Krivosheina, *Mod. Phys. Lett. A* **21**, 1547 (2006).
48. M. Agostini et al., *Nature* **544**, 47–52 (2017).
49. N. Abgrall et al., *Phys. Rev. Lett.* **118**, 161801 (2017).
50. C.E. Aalseth et al., *Phys. Rev. Lett.* **106**, 131301 (2011).
51. W. Zhao et al., *Phys. Rev. D* **93**, 092003 (2016).
52. R. Agnese et al., *Phys. Rev. D* **95**, 082002 (2017).
53. L. Hehn et al., *Eur. Phys. J C* **76**, 548 (2016).
54. M. Agostini et al., *Eur. Phys. J. C* **74**, 2764 (2014).
55. F. T. Avignone et al., *Nucl. Phys. B (Proc. Suppl.)* **28A**, 280 (1992).
56. H. Miley et al., *Nucl. Phys. B (Proc. Suppl.)* **28A**, 212 (1992).
57. H. V. Klapdor-Kleingrothaus et al., *Nucl. Instrum. Meth. A* **481**, 149 (2002).
58. E. B. Norman et al., *Nucl. Phys. B (Proc. Suppl.)* **143**, 508 (2005).
59. D. M. Mei et al., *Astropart. Phys.* **31**, 417–420 (2009).
60. S. R. Elliott et al., *Phys. Rev. C* **82**, 054610 (2010).
61. S. Cebrián et al., *Astropart. Phys.* **33**, 316–329 (2010).
62. G. Meierhofer et al., *Eur. Phys. J. A* **40**, 61 (2009).
63. G. Meierhofer et al., *Phys. Rev. C* **81**, 027603 (2010).
64. M. Bhike et al., *Phys. Lett. B* **741**, 150–154 (2015).
65. E. Armengaud et al., *Astropart. Phys.* **91**, 51–64 (2017).
66. B. White et al., Presentation at Low Radioactivity Techniques 2017 workshop, Seoul, Korea, <http://indico.ibs.re.kr/event/46/session/7/contribution/13>.
67. The Lund/LBNL Nuclear Data Search, <http://nucleardata.nuclear.lu.se/toi>
68. Decay Data Evaluation Project, <http://www.nucleide.org/DDEP.htm>
69. S. Cebrián et al., *Nucl. Phys. B (Proc. Suppl.)* **138**, 147–149 (2005).
70. E. Fascione and W. Rau, Cosmogenic Background in CDMSlite, Poster at the XV International Conference on Topics in Astroparticle and Underground Physics (TAUP 2017), Sudbury, Canada, <https://indico.cern.ch/event/606690/contributions/2591554/>.
71. J. Amaré et al., Cosmogenic production of tritium in dark matter detectors, arXiv:1706.05818v1 [physics.ins-det].
72. S. Jian et al., *Nucl. Instrum. Meth. A* **763**, 364–371 (2014).
73. A. Aguilar-Arevalo et al., *Phys. Rev. D* **94**, 082006 (2016).
74. A. Aguilar-Arevalo et al., *JINST* **10**, P08014 (2015).
75. C. Alduino et al., *Eur. Phys. J. C* **77**, 13 (2017).
76. S. Andringa et al., *Advances in High Energy Physics* **2016**, 6194250 (2016).
77. A. F. Barghouty et al., *Nucl. Instrum. Meth. B* **295**, 1621 (2013).
78. D.W. Bardayan et al., *Phys. Rev. C* **55**, 820 (1997).
79. B.S. Wang et al., *Phys. Rev. C* **92**, 024620 (2015).

80. C. Alduino et al., The projected background for the CUORE experiment, arXiv:1704.08970v1 [physics.ins-det].
81. V. Lozza and J. Petzoldt, *Astropart. Phys.* **61**, 62–71 (2015).
82. R. Bernabei et al., *Eur. Phys. J. C* **73**, 2648 (2013).
83. P. Adhikari et al., *Eur. Phys. J. C* **76**, 185 (2016).
84. E. Barbosa de Souza et al., *Phys. Rev. D* **95**, 032006 (2017).
85. J. Amaré et al., *J. Phys.: Conf. Ser.* **718**, 042052 (2016).
86. E. Shields et al., *Physics Procedia* **61**, 169 (2015).
87. K. Fushimi et al., *J. Phys.: Conf. Ser.* **718**, 042022 (2016).
88. G. Angloher et al., *Eur. Phys. J. C* **76**, 441 (2016).
89. J. Amaré et al., *JCAP* **02**, 046 (2015).
90. W.C. Pettus, *Cosmogenic Activation in NaI Detectors for Dark Matter Searches*, PhD thesis, University of Wisconsin-Madison, 2015.
91. G.J. Alner et al., *Phys. Lett. B* **616**, 17 (2005).
92. R. Bernabei et al., *Nucl. Instrum. Meth. A* **592**, 297–315 (2008).
93. R. Bernabei et al., *Int. J. Mod. Phys. A* **31**, 1642002 (2016).
94. G. Adhikari et al., *Eur. Phys. J. C* **77**, 437 (2017).
95. J. Amaré et al., *Eur. Phys. J. C* **76**, 429 (2016).
96. E. Aprile et al., *First Dark Matter Search Results from the XENON1T Experiment*, arXiv:1705.06655 [astro-ph.CO].
97. The LUX-ZEPLIN (LZ) Collaboration, *The LUX-ZEPLIN (LZ) Technical Design Report*, arXiv:1703.09144v1 [physics.ins-det].
98. A. Tan et al., *Phys. Rev. Lett.* **117**, 121303 (2016).
99. K. Abe et al., *Phys. Lett. B* **759**, 272–276 (2016).
100. M.G. Marino, *Nature* **510**, 229–234 (2014).
101. KamLAND-Zen Collaboration, *Phys. Rev. Lett.* **117**, 082503 (2016).
102. J. Martin-Albo et al., *JHEP* **05**, 159 (2016).
103. L. Baudis et al., *Eur. Phys. J. C* **75**, 485 (2015).
104. D.S. Akerib et al., *Astropart. Phys.* **62**, 33–46 (2015).
105. J.B. Albert et al., *JCAP* **04**, 029 (2016).
106. L. Giot et al., *Nucl. Phys. A* **899**, 116–132 (2013).
107. J. Calvo et al., *JCAP* **03**, 003 (2017).
108. P. Agnes et al., *Phys. Rev. D* **93**, 081101 (2016).
109. P.A. Amaudruz et al., *Nuclear and Particle Physics Proceedings* **273**, 340–346 (2016).
110. F.J. Iguaz et al., *Eur. Phys. J. C* **76**, 529 (2016).
111. P. Benetti et al., *Nucl. Instrum. Meth. A* **574**, 83–88 (2007).
112. J. Xu et al., *Astropart. Phys.* **66**, 53–60 (2015).
113. M. Labustenstein, G. Heusser, *App. Rad. Isot.* **67**, 750–754 (2009).
114. I. Coarasa et al., *Journal of Physics: Conference Series* **718**, 042049 (2016).
115. V.E. Guiseppe et al., *Astropart. Phys.* **64**, 34–39 (2015).
116. W. Maneschg et al., *Nucl. Instrum. Meth. A* **593**, 448–453 (2008).
117. D.S. Akerib et al., *Radio-assay of titanium samples for the LUX experiment*, arXiv:1112.1376 [physics.ins-det].
118. D.S. Akerib et al., *Identification of Radiopure Titanium for the LZ Dark Matter Experiment and Future Rare Event Searches*, arXiv:1702.02646v4 [physics.ins-det].
119. R. Strauss et al., *JCAP* **06**, 030 (2015).
120. R. Bernabei et al., *Int. J. Mod. Phys. A* **31**, 1642003 (2016).
121. O. Lebeda et al., *Phys. Rev. C* **85**, 014602 (2012).
122. O. Lebeda et al., *Nucl. Phys. A* **929**, 129–142 (2014).
123. J. S. O’Connell and F. J. Schima, *Phys. Rev. D* **38**, 2277–2279 (1988).

124. T. Hagner et al., *Astropart. Phys.* **14**, 33–47 (2000).
125. C. Galbiati et al., *Phys. Rev. C* **71**, 055805 (2005).
126. S. Abe et al., *Phys. Rev. C* **81**, 025807 (2010).
127. G. Bellini et al., *JCAP* **08**, 049 (2013).
128. D. Barker et al., *Phys. Rev. D* **86**, 054001 (2012).
129. L. Pandola et al., *Nucl. Instrum. Meth. A* **570**, 149–158 (2007).
130. A. Chilug, *Romanian Reports in Physics* **66**, 1200–1206 (2014).